

Sphere packing, helices and the polytope $\{3, 3, 5\}$

E.A. Lord^a and S. Ranganathan

Dept. of Metallurgy, Indian Institute of Science, Bangalore 560 012, India

Received 27 March 2001

Abstract. The packing of tetrahedra in face contact is well-known to be relevant to atomic clustering in many complex alloys. We briefly review some of the structures that can arise in this way, and introduce methods of dealing with the geometry of the polytope $\{3, 3, 5\}$, which is highly relevant to an understanding of these structures. Finally, we present a method of projection from S_3 to E_3 that enables coordinates for the key vertices of the collagen model of Sadoc and Rivier to be calculated.

PACS. 36.40.-c Atomic and molecular clusters – 87.15.-v Biomolecules: structure and physical properties

1 Introduction: sphere clusters and tetrahedron packing

Four equal spheres can be placed so that each touches the other three. The regular tetrahedron whose vertices are the sphere centres then has 0.7796... of its volume occupied by portions of the spheres. This gives the Rogers bound [1] – an absolute upper bound to the density of any possible packing of equal spheres in Euclidean 3-space. It is unattainable because regular tetrahedra do not pack together without gaps. The densest packing of equal spheres is the well-known hexagonal close packing, with density 0.7405...

Motivated by the need to understand the atomic structure of various complex transition metal alloys – now known as “Frank-Kasper phases” –, Frank and Kasper [2,3] investigated the possibilities of space filling by “almost regular” tetrahedra. The dihedral angle of a regular tetrahedron is about 70.5° , so that five of them can share a single edge, leaving only a small gap which can be closed by reducing the length of the common edge until the dihedral angle at this edge becomes 72° . We then have a *pentagonal bipyramid* with ten equilateral triangular faces. Replacing the five tetrahedra by centred truncated tetrahedra, the resulting cluster is one that has been identified as a structural subunit in many alloys with large unit cells [4–7]. Similarly, twelve regular tetrahedra can share a single vertex; the gaps between them can be closed by a slight deformation. We get a *regular icosahedron* (whose centre to vertex distance is 0.951... of the edge length, so the deformation of the tetrahedra is quite slight). This corresponds, in the Frank-Kasper phases, to a central atom coordinated to twelve others. Coordination numbers 14, 15 and 16 correspond to triangular-faced polyhedra built from tetrahedra sharing a single vertex (13

is not possible); the atoms in Frank-Kasper phases are located at the vertices and centres of various space filling arrangements of these polyhedra.

The *duals* of these structures are obtained by joining centres of every pair of tetrahedra in face contact. We get space-fillings by polyhedra with 12, 14, 15 and 16 faces (12 pentagons and 0, 2, 3 and 4 hexagons, respectively). They are the Voronoi regions of the vertices of the Frank-Kasper structures. Periodic structures with atoms at the vertices of these dual space fillings occur in clathrate hydrates [8,9]. Figure 12-8 of Pauling [10] shows the hydrogen bond framework of chlorine hydrate as a spacefilling of pentagonal dodecahedra and 14-hedra. This particular polyhedron packing led Weaire and Phelan to their discovery of a minimal area foam with a smaller area per unit volume than the previously known “best” solution of Kelvin [11,12].

Further considerations in this direction lead to the investigation of other possible types of clusters of equal, or nearly equal, spheres, of relevance (or potential relevance) to the structure of materials. A pair of overlapping icosahedra (Fig. 1) constructed from 35 tetrahedra represents a 19-sphere cluster. This kind of cluster occurs in quasicrystals [13] and in crystalline structures with very large unit cells [14]. Extending the structure produces a tower of *pentagonal antiprisms* (Fig. 2). Observe the ten polygonal helices, five left-handed and five right-handed, that wind around the structure with period ten. A cluster of four icosahedra each overlapping the three others in this way is indicated in Figure 3. In this cluster every icosahedron shares a pentagonal bipyramid of five tetrahedra with each of the three others; a single tetrahedron in the middle is common to all four icosahedra. These clusters are the basic subunits γ -brass, in which they are arrayed on a bcc lattice [15,16]. The cluster is built from 53 tetrahedra and has 26 vertices (22 on the surface and four inside). With rather more deformation they can be overlapped so that

^a e-mail: lord@metalrg.iisc.ernet.in

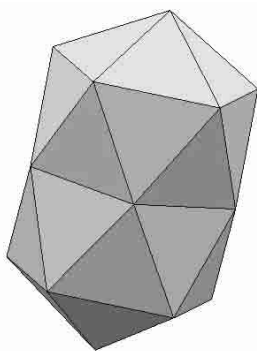


Fig. 1. The “double icosahedron” cluster.

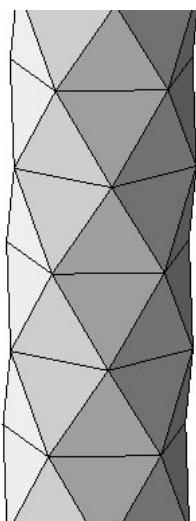


Fig. 2. Tower of pentagonal antiprisms.

each shares an icosahedron with four others. This gives rise to a *spacefilling* of irregular tetrahedra, corresponding to a Laves phase – a Frank-Kasper structure with coordination numbers 12 and 16. The vertices are located at the vertices of the space-filling of tetrahedra and truncated tetrahedra [9,17,18] and at the centres of the truncated tetrahedra. There are three edge lengths (bond lengths) in the ratio $\sqrt{2}:\sqrt{11}/2:\sqrt{3}$. The dual of the cluster is shown in Figure 4. It is a set of four pentagonal dodecahedra, slightly deformed so that each makes face contact with the other three (the face angle of a regular dodecahedron is 108° whereas the tetrahedral coordination angle required around the common vertex is $109.5\dots^\circ$, so the deformation is slight. With this face angle at two opposite vertices of the dodecahedral unit the structure can be extended to an open network of dodecahedra with the symmetry of the 4-connected diamond net. Figure 5 shows a portion of this structure. The remaining space can be filled by another “D network” of 16-faced polyhedra.

Pearce [18] observed that if four icosahedra are placed in face contact with a regular tetrahedron, they can be deformed slightly, becoming *oblate icosahedra*, so that each makes face contact with the other three (Fig. 6). There are 81 tetrahedra and 34 vertices. Observe that, whereas

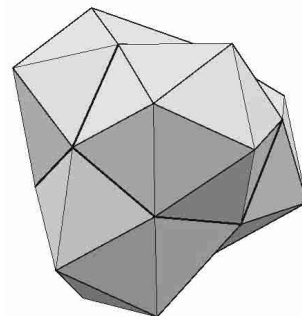


Fig. 3. Four interpenetrating icosahedra, sharing a central tetrahedron.

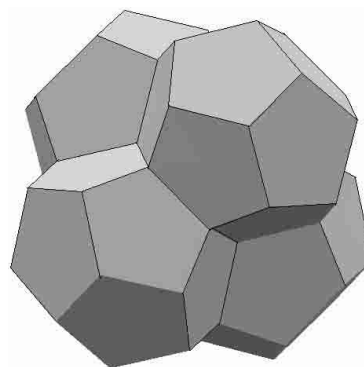


Fig. 4. Four pentagonal dodecahedra in face contact.

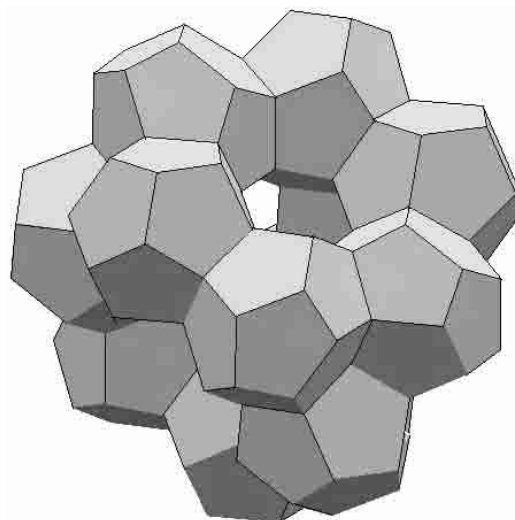


Fig. 5. Portion of the D-network of pentagonal dodecahedra.

in Figure 3 the icosahedra are twinned along fivefold axes, in the Pearce cluster they are twinned on threefold axes. These clusters occur in the Γ -phase of Fe–Zn, in which they are arrayed on a bcc lattice, each sharing three vertices with each of its eight neighbouring clusters [19]. The Pearce configuration can be extended to a D network open packing in which a regular tetrahedron is centred at each node and is linked to neighbouring nodes by oblate icosahedra (Fig. 7).

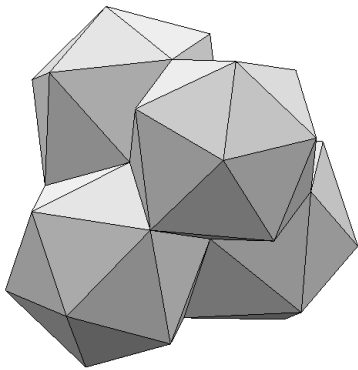


Fig. 6. The “Pearce” cluster; four icosahedra in face contact.

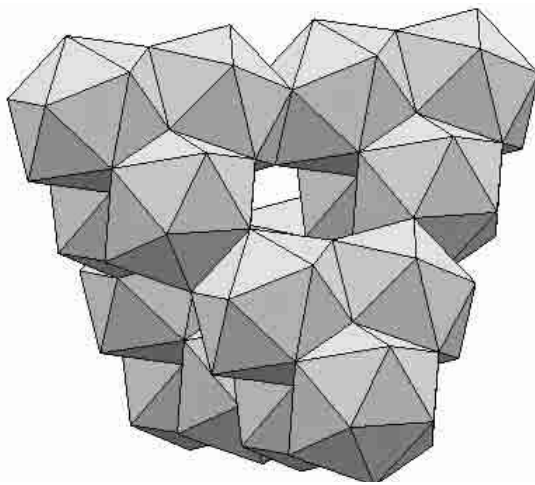


Fig. 7. A portipon of the D-network built from Pearce clusters.

Coxeter [20] suggested a straightforward extension of the concept of a *regular polygon*. A regular polygon as usually defined is a cycle of vertices $\dots 1, 2, 3, \dots$ and edges $\dots 12, 23, \dots$ obtained from a single point by repeated action of a rotation. Coxeter’s extension replaces “rotation” by the more general “isometry” (distance preserving transformation). A *screw transformation* generates a *helical polygon* (or *polygonal helix*), an infinite sequence of vertices $\dots -1, 0, 1, 2, \dots$ and edges joining consecutive vertices. A *Coxeter helix* is a polygonal helix such that every set of four consecutive vertices form a regular tetrahedron [21,22]. This produces a twisted rod of tetrahedra, the *Boerdijk-Coxeter helix* (Fig. 8) [23,24], on which three types of polygonal helix can be identified: the defining *Coxeter helix* $\dots 0, 1, 2, 3, \dots$ (a “type $\{1\}$ helix”), a double helix consisting of the polygons $\dots 0, 2, 4, 6, \dots$ and $\dots 1, 3, 5, 7, \dots$ (“type $\{2\}$ helices”), and a triple helix $\dots 0, 3, 6, 9, \dots$ and $\dots 1, 4, 7, 10, \dots$ and $\dots 2, 5, 8, 11, \dots$ (“type $\{3\}$ helices”).

The B-C helix is generated from a single regular tetrahedron by repeated application of a screw transformation. Other possibilities readily suggest themselves: Pearce [18] illustrated a helical packing of octahedra (Fig. 9) (its vertices are the mid-points of all the edges of a B-C helix) and one of icosahedra, Figure 10 (whose vertices are at golden mean positions on the edges of the helix of octahedra; it

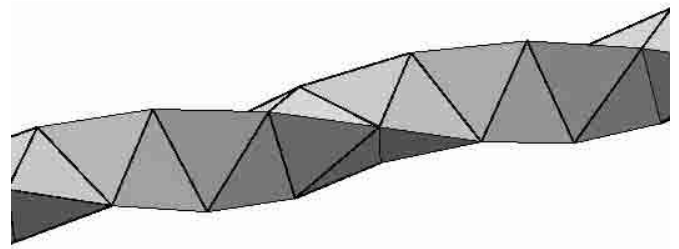


Fig. 8. The Boerdijk-Coxeter helix.

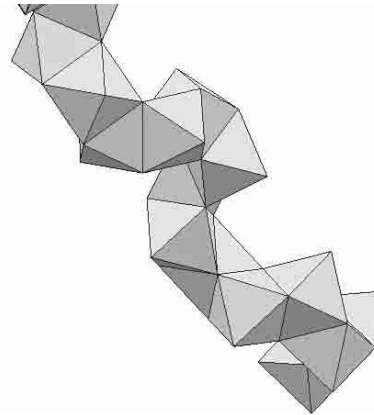


Fig. 9. A helix of octahedra.

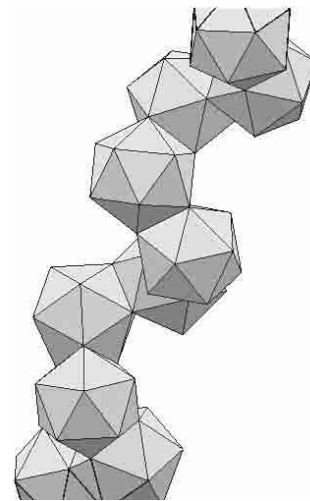


Fig. 10. A helix of icosahedra in face contact.

may also be arrived at by putting extra tetrahedra around a B-C helix). Figure 11 illustrates a helix of overlapping icosahedra in which every consecutive pair has the configuration shown in Figure 1.

2 Geometry of the B-C helix

In matrix notation, an isometry in Euclidean space has the form

$$\mathbf{x} \rightarrow R\mathbf{x} + \mathbf{a}, \quad RR^T = I. \quad (2.1)$$

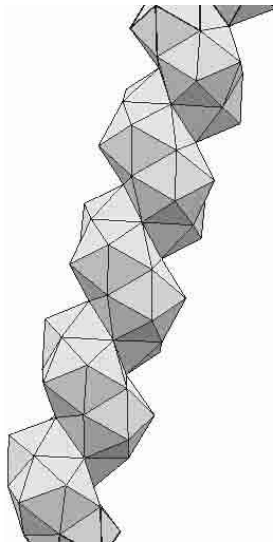


Fig. 11. A helix of interpenetrating icosahedra.

If $\mathbf{a} = \mathbf{0}$ we have a pure rotation about the origin. A rotation in E_3 through an angle θ about an axis along the unit vector \mathbf{n} is given by the rotation matrix

$$R = e^{\theta N} = I + N \sin \theta + N^2(1 - \cos \theta), \tag{2.2}$$

where N is the skewsymmetric matrix

$$N = \begin{pmatrix} 0 & -n_3 & n_2 \\ n_3 & 0 & -n_1 \\ -n_2 & n_1 & 0 \end{pmatrix}. \tag{2.3}$$

The right hand side of equation (2.2) is a consequence of the identity $N^3 = -N$.

It is convenient to use a 4×4 matrix notation. Defining

$$\mathbf{X} = \begin{pmatrix} \mathbf{x} \\ 1 \end{pmatrix}, \quad S = \begin{pmatrix} R & \mathbf{a} \\ 0 & 1 \end{pmatrix} \tag{2.4}$$

then equation (1) is

$$\mathbf{X} \rightarrow S\mathbf{X}. \tag{2.5}$$

The points in Euclidean 3-space with coordinates $(0\ 0\ 0)$, $(0\ 1\ 1)$, $(1\ 0\ 1)$ and $(1\ 1\ 0)$ are the vertices of a regular tetrahedron (edge length $\sqrt{2}$). So are $(0\ 1\ 1)$, $(1\ 0\ 1)$, $(1\ 1\ 0)$ and $(4/3\ 4/3\ 4/3)$. These can be taken to be two consecutive tetrahedra of a B-C helix. This is sufficient to deduce that

$$S = \begin{pmatrix} 0 & 1 & 1 & 4/3 \\ 1 & 0 & 1 & 4/3 \\ 1 & 1 & 0 & 4/3 \\ 1 & 1 & 1 & 1 \end{pmatrix} \begin{pmatrix} 0 & 0 & 1 & 1 \\ 0 & 1 & 0 & 1 \\ 0 & 1 & 1 & 0 \\ 1 & 1 & 1 & 1 \end{pmatrix}^{-1} = \frac{1}{3} \begin{pmatrix} 2 & 2 & 1 & 0 \\ 2 & -1 & -2 & 3 \\ -1 & 2 & -2 & 3 \\ 0 & 0 & 0 & 3 \end{pmatrix}.$$

From (2.1) we have

$$N \sin \theta = (R - R^T)/2, \quad \cos \theta = (1 + \text{tr}R)/2, \tag{2.6}$$

so that S gives us immediately, for the angle θ of rotation of the B-C helix (per edge of the type $\{1\}$ helix) and the direction \mathbf{n} of the screw axis,

$$\cos \theta = -1/3, \quad \mathbf{n} = [2\ 1\ 0]/\sqrt{5}. \tag{2.7}$$

The number of edges of the type $\{1\}$ helix, per turn, is $2\pi/\theta = 2.73119\dots$ The advance of the helix, per edge, is $\mathbf{n} \cdot \mathbf{d}$, where \mathbf{d} is any edge (*e.g.* $[0\ 1\ 1]$). Since we have chosen tetrahedra with edge length $\sqrt{2}$, we have the advance per edge, for a B-C helix of tetrahedra of unit edge length,

$$d = 1/\sqrt{10}.$$

An isometry in E_3 is determined if four non-coplanar points and their four images are given, so the method is applicable to other helical towers of identical polyhedra.

3 The polytope $\{3, 3, 5\}$

Perfectly regular tetrahedra can be packed together in a spherical space S_3 . On a hypersphere embedded in Euclidean space E_4 the vertices are those of the regular polytope $\{3, 3, 5\}$. It follows that various of the clusters discussed above, built from slightly irregular tetrahedra, exist in this polytope without any irregularity.

The polytope $\{3, 3, 5\}$ has 120 vertices, 720 edges, 1200 equilateral triangular faces and 600 regular tetrahedral cells [22]. There are 5 tetrahedra around every edge and twelve around every vertex (forming a regular icosahedron). From these facts, the information contained in the incidence matrix below is easily deduced. The off-diagonal element ij gives the number of $(j-1)$ -dimensional ‘‘facets’’ contained in or containing each $(i-1)$ -dimensional facet:

120	12	30	12
2	720	5	5
3	3	1200	2
4	6	4	600

A standard set of coordinates for the vertices is given by all the *even* permutations of

$$\begin{aligned} & \frac{1}{2} (\pm 2\ 0\ 0\ 0) \\ & \frac{1}{2} (\pm 1\ \pm 1\ \pm 1\ \pm 1) \\ & \frac{1}{2} (\pm \tau\ \pm 1\ \pm \sigma\ 0) \end{aligned} \tag{3.1}$$

where τ is the golden number, $\tau = (1 + \sqrt{5})/2$ and $\sigma = -\tau^{-1} = (1 - \sqrt{5})/2$ (*i.e.*, τ and σ are the roots of $\lambda^2 - \lambda - 1 = 0$). The radius of this $\{3, 3, 5\}$ is 1 and its edge length is $1/\tau$.

The vertices, of course, all lie on the *hypersphere* (S_3)

$$x_0^2 + x_1^2 + x_2^2 + x_3^2 = 1. \tag{3.2}$$

Table 1. Radii of successive shells around a vertex of {3, 3, 5}.

$2x_0$	n		d	$\cos \alpha$
2	1	“centre”	0	1
τ	12	icosahedron	$1/\tau$	τ
1	20	dodecahedron	1	$1/2$
$-\sigma$	12	icosahedron	$\sqrt{(3-\tau)}$	$1/2\tau$
0	30	icosidodecahedron	$\sqrt{2}$	0
σ	12	icosahedron	τ	$-1/\tau$
-1	20	dodecahedron	$\sqrt{3}$	$-1/2$
$-\tau$	12	icosahedron	$\sqrt{(2+\tau)}$	$-\tau/2$
-2	1	antipodal vertex	2	-1

Table 2. Coordinates of the vertices of the icosidodecahedral shell indicated in Figure 12.

1	2	3	4	5	6	7	8	9	10	11	12	13	14	15
$-\sigma$	1	τ	2	0	0	σ	1	τ	$-\sigma$	-1	τ	σ	-1	
τ	$-\sigma$	1	0	2	0	τ	σ	1	-1	τ	$-\sigma$	-1	τ	σ
1	τ	$-\sigma$	0	0	2	1	τ	σ	$-\sigma$	-1	τ	σ	-1	τ

In the spherical representation of the polytope the edges, faces and cells are projected onto this S_3 . The edges are then represented by arcs of *great circles*. A way of visualising the polytope is as follows [22]. Take a single vertex – for convenience, $(1\ 0\ 0\ 0)$ – as a “centre” and consider the successive “shells” of vertices that surround it. The first shell is an icosahedron, then 12 vertices lying over the faces of the first shell form a regular dodecahedron. The third shell is another, larger icosahedron. So far, the sequence is the same as the sequence of shells of atoms in the Bergman cluster [25]. The vertices of the next shell all lie on a *great sphere* of the S_3 (in the lower dimensional analogy, the “centre” would be, say, the north pole. We have arrived at the equator). This great sphere contains 30 vertices, forming an *icosidodecahedron* (i.e. the Archimedean polyhedron whose vertices are all the midpoints of edges of an icosahedron. Its triangular and pentagonal faces are arranged in the pattern (3.5.3.5) around the vertices). The sequence of shells thereafter goes in reverse order, till we reach $(-1\ 0\ 0\ 0)$ (the “south pole”). Table 1 gives, for each shell, the x_0 coordinate of its vertices, its distance d from the $(1\ 0\ 0\ 0)$ measured in E_4 , and its distance α measured in S_3 .

In the following section it will be convenient to have names (labels) for the vertices of the equatorial icosidodecahedron. Our labelling system is given by Table 2, which lists, for each vertex, the coordinates $2x_1, 2x_2, 2x_3$ (as a column).

The vertices diametrically opposite those listed may be denoted by attaching minus signs to the labels. The labelling of the icosidodecahedron is illustrated in Figure 12.

Observe that the edges and vertices of an icosidodecahedron lie on *six planar decagons*. In the spherical representation, these decagons are *great circles*. The {3, 3, 5} contains 72 of them – corresponding to 72 great circles in S_3 . It is not difficult to deduce that the vertices, great

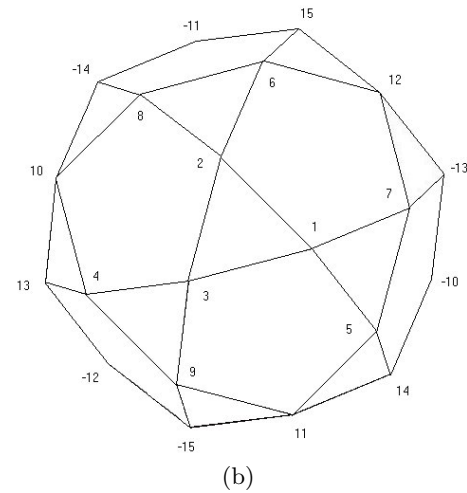
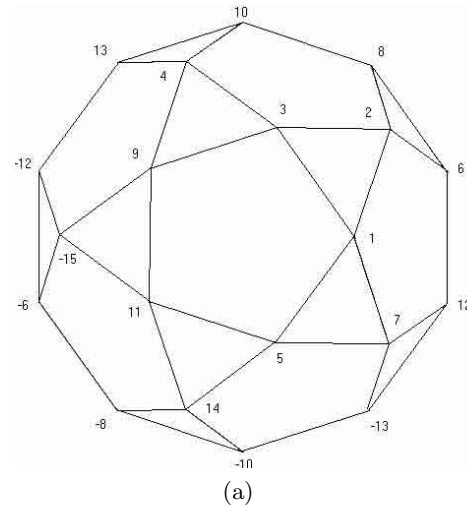


Fig. 12. The labeling of an equatorial icosidodecahedron of {3, 3, 5}. (a) View along 5-fold axis. (b) View along 3-fold axis.

circles and great spheres in the spherical representation of {3, 3, 5} constitute a configuration described by the following incidence matrix:

120	6	15
10	72	5
30	6	60

4 Rotations and double rotations in E_4

Euclidean transformations in E_4 about a fixed origin (equivalently, rotations of S_3) are most simply and elegantly expressed in terms of *quaternions*. “Real” quaternions are essentially sets of four real numbers $q = (q_0\ q_1\ q_2\ q_3) = (q_0, \mathbf{q})$, with the multiplication law

$$pq = (p_0q_0 - \mathbf{p} \cdot \mathbf{q}, \mathbf{p} \times \mathbf{q} + p_0\mathbf{q} + \mathbf{p}q_0). \tag{4.1}$$

The *conjugate* of a quaternion q is $\bar{q} = (q_0, -\mathbf{q})$, its *norm* is $q\bar{q} = \bar{q}q = q_0^2 + q_1^2 + q_2^2 + q_3^2$, and its *modulus* $|q|$ is the square root of the norm. The *unit quaternion* is $(1 \ 0 \ 0 \ 0)$ and every non-zero quaternion has an inverse $q^{-1} = \bar{q}/|q|$.

Writing the coordinates of points in E_4 as quaternions $x = (x_0 \ x_1 \ x_2 \ x_3) = (x_0, \mathbf{x})$, the Euclidean transformations, keeping the origin fixed are the *double rotations*

$$x \rightarrow pxq, \quad (4.2)$$

where p and q are quaternions of unit norm. The corresponding orthogonal 4×4 matrix is

$$R = PQ, \quad (4.3)$$

where

$$P = \begin{pmatrix} p_0 & -p_1 & -p_2 & -p_3 \\ p_1 & p_0 & p_3 & -p_2 \\ p_2 & -p_3 & p_0 & p_1 \\ p_3 & p_2 & -p_1 & p_0 \end{pmatrix}, \quad Q = \begin{pmatrix} q_0 & -q_1 & -q_2 & -q_3 \\ q_1 & q_0 & -q_3 & q_2 \\ q_2 & q_3 & q_0 & -q_1 \\ q_3 & -q_2 & q_1 & q_0 \end{pmatrix}.$$

The quaternions p and q can be written as

$$p = (\cos \theta, \mathbf{n} \sin \theta), \quad q = (\cos \varphi, \mathbf{m} \sin \varphi), \quad (4.4)$$

thus defining a useful set of parameters for the four-dimensional orthogonal group: two angles θ and φ and two unit 3-vectors \mathbf{n} and \mathbf{m} .

The special transformations of the form

$$x \rightarrow px, \quad \text{and} \quad x \rightarrow xq \quad (4.5)$$

are called, respectively, *left* and *right Clifford translations*. In their action on a hypersphere S_3 , centred at the origin of E_4 , they have *no fixed points* (this phenomenon has no analogue in E_3 : every rotation of a sphere S_2 has two fixed points). This observation leads to the concept of a *Hopf fibration* [16, 26] of S_3 . For any given point x in S_3 , a transformation $x \rightarrow px$ generates a *great circle* in S_3 , parametrised by the variable θ . For fixed \mathbf{n} , we can generate a great circle through *every* point x of S_3 . This set of circles constitute a *left Hopf fibration*. Obviously, no two of the circles can intersect. In fact, every pair of circles is linked! The circles are the *fibres* of the fibration. Similarly, *right Hopf fibrations* are defined in terms of the transformations $x \rightarrow xq$.

5 Rotational symmetries of $\{3, 3, 5\}$

The symmetries of $\{3, 3, 5\}$ are transformations of the form (4.3) for which the components of p and q are permutations of the coordinate sets (3.1). We get a group of order 7200. (The full symmetry group including reflections has order 14400). It is a strange property of the polytope $\{3, 3, 5\}$ that the quaternions representing its vertices are the same quaternions that represent its symmetries. Even more odd is that the rows and columns of the 7200 matrices R are the same 120 4-vectors!

The 120 vertices of $\{3, 3, 5\}$ lie in tens on 12 great circles, which are twelve circles of a Hopf fibration. In fact, the vertices can be assigned in tens to twelve fibres, in 24 different ways (corresponding to 12 left and 12 right fibrations). Consider, for definiteness, the effect of the left translation $p \rightarrow px$ with

$$p = \frac{1}{2}(\tau - \sigma \ 1 \ 0), \quad (5.1)$$

(i.e., $\theta = \pi/5$ and $\mathbf{n} \sim [1 \ \tau \ 0]$) on the vertices of the polytope. In matrix formulation, we have the repeated action of the corresponding orthogonal matrix

$$R = \frac{1}{2} \begin{pmatrix} \tau & \sigma & -1 & 0 \\ -\sigma & \tau & 0 & -1 \\ 1 & 0 & \tau & -\sigma \\ 0 & 1 & \sigma & \tau \end{pmatrix} \quad (5.2)$$

on the position vectors. Since $p^5 = -1$, R has order 10, so it generates decagons. The repeated action of R on any vertex of the polytope generates a decagon of vertices lying on a fibre.

The twelve fibres can be visualised in terms of a stereographic projection of S_3 to E_3 . Since E_3 is the space in which we live, configurations in it are more easily imagined. Moreover, circles in S_3 are mapped to circles (or straight lines) in E_3 and spheres are mapped to spheres (or planes). Let us project from $(-1 \ 0 \ 0 \ 0)$ to the hyperplane (E_3) $x_0 = 0$.

Starting from vertex **6** $(0 \ 0 \ 0 \ 1)$ and applying the transformation R repeatedly we get the sequence of ten vertices around the perimeter of Figure 12b – lying on a great circle **A**. Starting from $(1 \ 0 \ 0 \ 0)$ we get a great circle **B** – which in the stereogram is a line perpendicular to the page passing through the middle of the figure, containing none of the vertices of the icosidodecahedron. The remaining 10 fibres are obtained by repeated application of R to the remaining ten vertices of the icosidodecahedron. They are circles that pass through a pair of diametrically opposite vertices of the icosidodecahedron.

Similarly, a fibration $x \rightarrow xq$ with $\varphi = \pi/3$ (so that $q^3 = -1$) gives a transformation of order six that assigns the 120 vertices of the polytope to 20 fibres with six vertices on each. The hexagon edges, however, are not edges of the $\{3, 3, 5\}$.

6 The Boerdijk-Coxeter helices in $\{3, 3, 5\}$

Consider the effect of repeated action of

$$x \rightarrow p^2 xq \quad (6.1)$$

with $p = 1/2(\tau - \sigma \ 1 \ 0)$, $q = 1/2(1 \ 1 \ 1 \ 1)$; i.e., $\theta = \pi/5$, $\varphi = \pi/3$, $\mathbf{n} \sim [1 \ \tau \ 0]$, $\mathbf{m} \sim [1 \ 1 \ 1]$. Then

$$R = \frac{1}{2} \begin{pmatrix} -1 & -\tau & \sigma & 0 \\ 0 & -\sigma & -\tau & -1 \\ \tau & -1 & 0 & \sigma \\ -\sigma & 0 & -1 & \tau \end{pmatrix}. \quad (6.2)$$

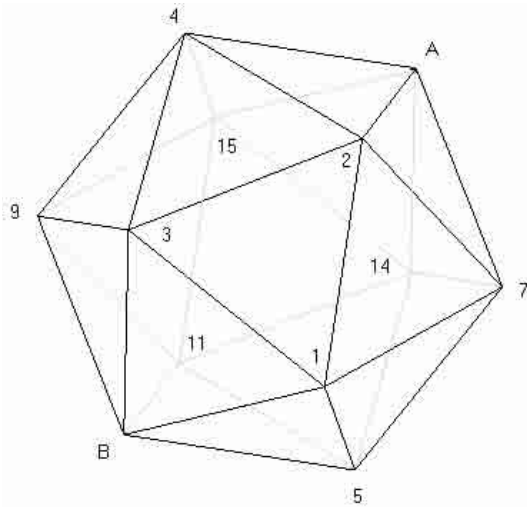


Fig. 13. Representation of the configuration of twelve fibres of a Hopf fibration.

Since $p^5 = q^3 = -1$, R has order 30. It will generate a sequence of 30 vertices (an orbit of the transformation R), starting from any vertex of $\{3, 3, 5\}$. For example, starting from **6** (0 0 0 1) we get the the vertices given by the columns of

$$\frac{1}{2} \begin{pmatrix} 0 & 0 & 1 & 0 & -\sigma & 1 & 0 & 1 & -\sigma & 0 & 1 & 0 & 0 & -\sigma & \sigma \\ 0 & -1 & \sigma & -1 & -\tau & -1 & -\tau & -\tau & -1 & -\tau & -1 & \sigma & -1 & 0 & 0 \\ 0 & \sigma & 0 & -\sigma & 0 & 1 & 1 & -\sigma & \tau & 1 & 1 & \tau & -\sigma & 1 & 1 \dots \\ 2 & \tau & \tau & \tau & 1 & 1 & -\sigma & 0 & 0 & \sigma & -1 & -1 & -\tau & -\tau & -\tau \end{pmatrix}$$

(... denotes a repetition of the fifteen given columns, with opposite sign.) in this sequence, every set of four consecutive vertices is the set of vertices of a regular tetrahedron with edge length $1/\tau$. That is, we have a *Boerdijk-Coxeter helix* consisting of 30 tetrahedral cells of $\{3, 3, 5\}$.

The geometrical situation can be explored further. The fibres of a Hopf fibration are *parallel* (i.e., any two maintain a constant S_3 distance from each other). Each of the twelve fibres associated with the decagons of $\{3, 3, 5\}$ has five nearest neighbours. Figure 13 is a representation of this nearest neighbour relationship. The twelve fibres are represented as the twelve vertices of an icosahedron and the icosahedron edges represent the nearest neighbour relationship. (N.B.: this icosahedron has nothing to do with the icosahedral shells of the polytope. In the mathematical terminology it is the *base space* of the *fibre bundle* [26].) For every triangular face of this icosahedron there is a B-C helix whose type $\{3\}$ helices are three decagons of the polytope. Thus $\{3, 3, 5\}$ consists of twenty toroidal B-C helices packed together, wrapped around each other.

7 The collagen molecule as four B-C helices: the Sadoc-Rivier model

Sadoc and Rivier [27] have recently suggested a fascinating model for the structure of collagen. Their claim is that the

central core of hydrogen bonds is essentially a B-C helix – thus, a close-packing arrangement – formed by wrapping three peptide chains around it. The covalent “backbones” of these peptide chains are themselves type $\{2\}$ helices of three B-C structures twisted around each other like the strands of a rope. Sadoc and Rivier describe the configuration in terms of the properties of $\{3, 3, 5\}$ that we have described above.

The structure can be represented in $\{3, 3, 5\}$ by four B-C structures such as **123**, **157**, **2A4** and **39B** in Figure 13. When this is mapped to E_3 , the fact that the type $\{2\}$ and type $\{1\}$ helices of a B-C structure are oppositely handed corresponds to the fact that the peptide chains in collagen are left-handed and twist around each other in a right-handed sense [28]. Identifying them with type $\{2\}$ helices also fits well with the observed pitch of the polyproline helix, which is about twice that of a type $\{1\}$ Coxeter helix.

8 Mapping S_3 to E_3

Close-packed arrangements of equal spheres has a perfection in S_3 that is impossible in E_3 . The various clusters built from irregular tetrahedra, discussed in Section 1, or the equivalent clusters of equal or nearly equal spheres, exist in S_3 without any irregularity. To obtain realistic models of E_3 structures from the elegant geometry of $\{3, 3, 5\}$ the polytope has to be mapped in some way, by “unfolding” it or by a projection method [29–33].

The problem is analogous to the problem traditionally faced by cartographers, whose task is to map S_2 (the surface of the earth) to E_2 (the page of an atlas). Distortion is inevitable. The projection method employed in any particular case is chosen to preserve some particular property, dictated by the purpose of the map.

Spherical space S_3 can be parametrised by three angular variables (analogous to longitude and latitude, for S_2):

$$\begin{aligned} x_0 &= \sin \Theta \cos \Phi, & x_1 &= \cos \Theta \cos \Psi, \\ x_2 &= \cos \Theta \sin \Psi, & x_3 &= \sin \Theta \sin \Phi. \end{aligned} \quad (8.1)$$

Observe that $\Phi \rightarrow \Phi + \alpha$ is a rotation in the (0 3)-plane and $\Psi \rightarrow \Psi + \beta$ is a rotation in the (1 2)-plane. In terms of quaternions, these transformations are respectively $x \rightarrow pxp$ and $x \rightarrow px\bar{p}$, with $p = (\cos(\alpha/2), 0, 0, \sin(\alpha/2))$. It follows that, in terms of these polar coordinates,

$$\Phi \rightarrow \Phi + \gamma, \quad \Psi \rightarrow \Psi - \gamma \quad (8.2)$$

is a *left Clifford translation* and

$$\Phi \rightarrow \Phi + \gamma, \quad \Psi \rightarrow \Psi + \gamma \quad (8.3)$$

is a *right Clifford translation*. (In terms of quaternions, $x \rightarrow px$ and $x \rightarrow xq$, respectively, with p or q of the form $(\cos \gamma, 0, 0, \sin \gamma)$).

To obtain a realistic model for the collagen structure by projection from the corresponding structure in $\{3, 3, 5\}$ a mapping is required that maps great circles of a Hopf

fibration of S_3 to *helices* in E_3 . In terms of the polar coordinate system given by (8.1), a mapping with this property exists that has a remarkably simple form. Let ρ, φ, z be the coordinates of a cylindrical coordinate system in E_3 . Then the mapping from S_3 to E_3 given by

$$\rho = \Theta, \quad \varphi = \Phi, \quad z = -\Psi \quad (8.4)$$

has the following properties. The fibres of the left translation (8.2) all lie on toruses $\Theta = \text{const.}$ and are mapped to helices that wind around the z -axis (which is itself the image of the fibre $\Theta = 0$). Distances along the z -axis and radial distances from the z -axis represent accurately the corresponding distances in S_3 . The projection is a generalisation to higher dimensions of *Mercator's projection* from S_2 to E_2 , which represents distances along the equator and along lines of longitude accurately to scale, while stretching out of lines of latitude increases in severity as one moves away from the equator.

We now choose the position of a $\{3, 3, 5\}$ in S_3 so that all the vertices of one of its B-C helices lie on a torus $\Theta = \text{const.}$ (and hence the projected vertices in E_3 all lie on a cylinder whose axis is the z -axis). The minus sign in (8.4) ensures that the type $\{1\}$ helix will be right-handed.

We have seen that the 30 vertices of a type $\{1\}$ helix in S_3 are generated by a transformation P^2Q , where P is a left translation with angular parameter $\pi/5$ and Q is a right translation with angular parameter $\pi/3$. It follows from the prescriptions (8.2, 8.3), that such a transformation is given by

$$\Phi \rightarrow \Phi + 11\pi/15, \quad \Psi \rightarrow \Psi - \pi/15. \quad (8.5)$$

The image of a point $(\Theta, \Phi, \Psi) = (\Theta_1, 0, 0)$ is $(\Theta_1, 11\pi/15, -\pi/15)$. If these are two vertices of an edge of $\{3, 3, 5\}$ their S_3 distance must be $\cos^{-1}(\tau/2)$. This gives

$$\tau/2 = \sin^2 \Theta_1 \cos(11\pi/15) + \cos^2 \Theta_1 \cos(\pi/15),$$

and hence

$$\cos \Theta_1 = \sqrt{\frac{1}{2} \left(1 + \frac{\tau^2}{\sqrt{3(2+\tau)}} \right)}. \quad (8.6)$$

This enables the polar coordinates of all the vertices of a B-C helix in $\{3, 3, 5\}$ (and hence their images in E_3) to be computed. To identify the positions of other vertices of this $\{3, 3, 5\}$ we proceed as follows:

Let v_1, v_2, v_3, v_4 be the E_4 position vectors of the vertices of any tetrahedral cell of our $\{3, 3, 5\}$ and let v_5 be the position vector of the remaining vertex of the adjoining cell, sharing the face (v_1, v_2, v_3) . Then

$$v_5 = (v_1 + v_2 + v_3)/\tau - v_4. \quad (8.7)$$

(Observe, incidentally, that the corresponding formula for a pair of tetrahedra lying in E_3 is $v_5 = \frac{2}{3}(v_1 + v_2 + v_3) - v_4$. To produce the polytope, contiguous tetrahedra are rotated about their common face – just as, in making a model of an icosahedron from a flat net, we have to rotate neighbouring triangles about their common edge.)

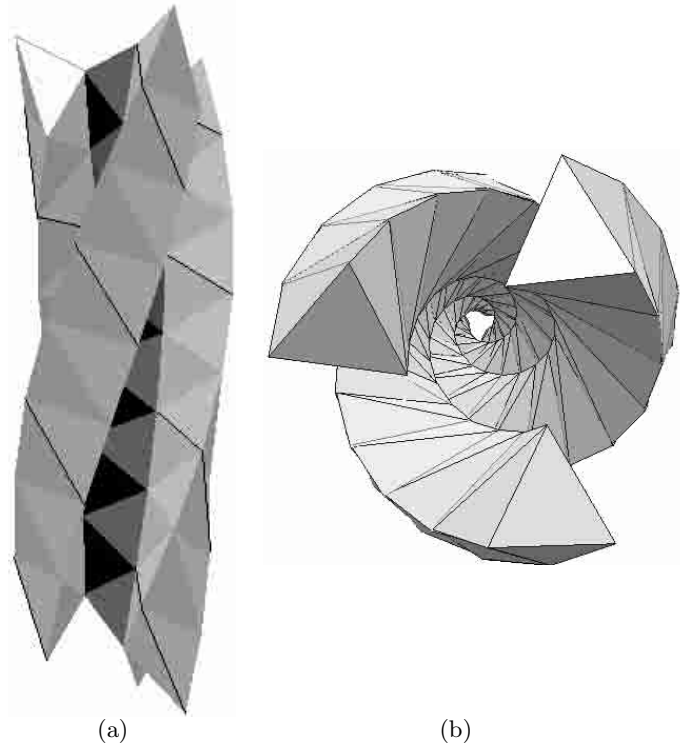


Fig. 14. Illustration of the collagen model of Sadoc and Rivier, produced by our projection method. Three columns of packed tetrahedra twist around a central B-C helix. The type $\{2\}$ helices marked in black correspond to the peptide chains. (a) General view of the four B-C helices. (b) Perspective view along the axis.

In principle, the positions of all 120 vertices of a $\{3, 3, 5\}$ can be computed from this formula, if the positions of the three vertices of a single triangular face are given.

The central type $\{1\}$ helix obtained by the projection of $\{3, 3, 5\}$ employing (8.4) is an almost exact Coxeter helix: the number of edges per turn is $30/11 = 2.727$, instead of 2.731. The structure is periodic – the type $\{3\}$ helix has exactly 10 edges per turn. a slight “untwisting” of this structure is still required if a realistic model of the collagen model is to be obtained. We apply a further transformation of the form $\varphi \rightarrow \varphi + kz$. the parameter k adjusts the pitch of the type $\{3\}$ helices of the central B-C structure, and is chosen so that about ten glycines per turn occur along each type $\{3\}$ helix of the core, as in the actual molecule. This untwisting transformation introduces very slight additional deformation of the central B-C helix, but *lessens* the inevitable distortion of the three outer B-C helices.

The illustrations of the geometrical basis for the Sadoc-Rivier collagen model, shown in Figure 14, resulted from computation based on (8.6, 8.7), and the mapping (8.4), followed by the untwisting transformation. The coordinates were calculated for just seven vertices of the structure, corresponding to a tetrahedron of the core and two belonging to outer structure. All other vertices are

obtained by applying a screw transformation. The 3D graphics facility of Brakke's software "Surface Evolver" [34] produced the pictures.

References

1. J.H. Conway, N.J.A. Sloane, *Sphere Packings, Lattices and Groups* (Springer, London and New York, 1988).
2. F.C. Frank, J.S. Kasper, *Acta Cryst.* **11**, 184 (1958).
3. F.C. Frank, J.S. Kasper, *Acta Cryst.* **12**, 483 (1959).
4. S. Samson, *Acta Cryst. A* **11**, 851 (1958).
5. S. Samson, *Acta Cryst. A* **14**, 1229 (1961).
6. S. Samson, *Acta Cryst. A* **17**, 491 (1964).
7. S. Samson, *Acta Cryst. A* **19**, 401 (1965).
8. K.W. Allen, *J. Chem. Phys.* **41**, 840 (1964).
9. R. Williams, *The Geometrical Foundation of Natural Structure* (Endaeum Press, Marpark Calif. 1972; Dover, New York, 1979).
10. L. Pauling, *The Nature of the Chemical Bond*, 3rd edn. (Cornell University Press, 1960).
11. D. Weaire, R. Phelan, *Phil. Mag. Lett.* **69**, 107 (1994).
12. N. Rivier, *Phil. Mag. Lett.* **69**, 297 (1994).
13. D. Romeu, J.L. Aragon, in *Crystal-Quasicrystal Transitions*, edited by M.J. Yacaman, M. Torres (Elsevier, 1993).
14. G. Kreiner, H.F. Franzen, *J. Alloys Comp.* **221**, 15 (1995).
15. A.J. Bradley, P. Jones, *J. Inst. Met.* **51**, 131 (1933).
16. J.F. Sadoc, R. Mosseri, *Frustration Géométrique* (Eyroles, Paris, 1997); *Geometrical Frustration* (Cambridge University Press, 1999).
17. K. Critchlow, *Order in Space* (Thames and Hudson, London, 1969).
18. P. Pearce, *Structure in Nature is a Strategy for Design* (MIT Press, 1990).
19. C.H.E. Belin, R.C.H. Belin, *J. Solid State Chem.* **151**, 85 (2000).
20. H.S.M. Coxeter, *Regular Complex Polytopes* (Cambridge University Press, 1974).
21. H.S.M. Coxeter, *Introduction to Geometry*, 4th edn. (John Wiley & Sons, 1961).
22. H.S.M. Coxeter, *Regular Polytopes* (Macmillan, 1963; Dover, 1973).
23. A.H. Boerdijk, *Philips Res. Rep.* **7**, 303 (1952).
24. H.S.M. Coxeter, *Can. Math. Bull.* **28**, 385 (1985).
25. G. Bergman, J.L.T. Waugh, L. Pauling, *Acta Cryst.* **10**, 254 (1957).
26. N. Steenrod, *The Topology of Fiber Bundles* (Princeton University Press, 1951).
27. J.F. Sadoc, N. Rivier, *Eur. Phys. J. B* **12**, 309 (1999).
28. A.L. Lehninger, D.L. Nelson, M.M. Cox, *Principles of Biochemistry* (Worth Publishers, New York, 1993).
29. M. Kléman, J.F. Sadoc, *J. Phys. France Lett.* **40**, L569 (1979).
30. D.R. Nelson, *Phys. Rev. Lett.* **50**, 982 (1983).
31. J.F. Sadoc, *J. Phys. France Lett.* **44**, L707 (1983).
32. J.F. Sadoc, R. Mosseri, *J. Phys. France* **46**, 1809 (1985).
33. J.F. Sadoc, N. Rivier, *Phil. Mag. B* **55**, 537 (1987).
34. K.A. Brakke, *Exp. Math.* **1**, 141 (1992).